Astron. Astrophys. 317, 942–948 (1997)

ASTRONOMY
AND
ASTROPHYSICS

High spatial-resolution spectropolarimetry of small-scale solar magnetic fields

F. Stolpe and F. Kneer

Universitäts-Sternwarte, Geismarlandstr. 11, D-37083 Göttingen, Germany

Received 25 March 1996 / Accepted 13 June 1996

Abstract. We present a study of the structure and the dynamics of small-scale magnetic elements within solar plage regions. Spectropolarimetric observations with high spatial and spectral resolutions have been obtained for three iron lines with different sensitivities to magnetic field strength and temperature with the Gregory Coudé Telescope at the Observatorio del Teide/Tenerife. The main results are:

1. With the present spatial resolution of $0\farcs6$–$1\farcs0$, the continuum intensity from magnetic areas is close to the average intensity of the quiet Sun ($\pm 5\%$). There is a slight tendency of decreasing intensity with increasing magnetic flux within the resolution elements.
2. Macroscopic velocities with rms values of 1.5–2.0 km s^{-1} as used to explain the widths of the Stokes V profiles are not seen with the spatial resolution obtained here.
3. The large observed fluctuations in the wavelength separation of the red and blue Stokes V maxima suggest that there may be a considerable variation in the properties of the flux tubes.

This should give constraints for modeling small-scale flux tubes.

Key words: Sun: plages – Sun: magnetic fields – small-scale magnetic flux tubes, observation of

1. Introduction

Small-scale magnetic flux tubes are an essential ingredient for the structure and the dynamics of the solar atmosphere. They constitute a substantial part of the magnetic flux which emerges from the solar surface. They are almost ubiquitous, found not only in active regions but also in the quiet Sun at downdrafts (Stenflo 1973). Small-scale magnetic elements are also intimately related to bright structures and highly dynamic processes in the chromosphere and corona of the Sun (the reader is referred to Ulmschneider et al. (1991), Solanki (1993, 1995), or Stenflo (1994) and to further references there). They possess several hundred mT fields (e.g. Beckers & Schröter 1968) and have diameters at the base of the solar photosphere ($\tau_{5000} = 1$) of at most a few 100 km, i.e. at the lower limit of what modern solar telescopes can resolve. Much of the properties of small-scale flux tubes are derived, by indirect ways, from observations with low spatial resolution (e.g. Solanki & Stenflo 1984, 1985). Spectropolarimetric observations with high spatial resolution are rare. Fleck & Deubner (1991) presented the analysis of a time sequence of Stokes V profiles with high spatial resolution with emphasis on the temporal evolution of flux tubes. Keller & von der Lühe (1992) could confirm the smallness of magnetic elements, by combining broad-band polarimetry with speckle methods. Volkmer et al. (1995), performing two-dimensional spectropolarimetry with both high spatial and high wavelength resolution, could follow the horizontal migration of flux tubes and found for the first time short-period (100 s) oscillations in small-scale elements.

Very recently, Martínez Pillet et al. (1996) performed an analysis of full Stokes vector data with a spatial resolution of about $1''$ from active regions on the Sun obtained with the Advanced Stokes Polarimeter at Sacramento Peak Observatory. By means of an inversion code, they derived such parameters as magnetic field strength, field orientation with respect to the solar surface, and filling factors in small-scale magnetic features. They also put much emphasis on the centre to limb variation of field strength, the velocity of the magnetic plasma, and the Stokes V, Q, and U profile asymmetries.

In this contribution, we continue the efforts by Amer & Kneer (1993) and present spectropolarimetric observations with high spatial resolution. Although spatial averaging is not avoidable due to limited telescopic resolution and to seeing it is substantially reduced compared with e.g. data from the Fourier Transform Spectrometer. High resolution observations give detailed views on the state and dynamic behaviour of the magnetized plasma and may be used for a comparison with the radiation calculated from models of flux tubes.

2. Observations

The observations consist of spectropolarimetric measurements from plage regions near disc centre of the Sun obtained with

Send offprint requests to: F. Stolpe

the Gregory Coudé Telescope (Kneer et al. 1987) at the Observatorio del Teide/Tenerife on August 25 and September 3, 1992, under good seeing conditions. A Stokes V polarimeter, consisting of a $\lambda/4$ retarder and two crossed calcite rods, was mounted behind the entrance slit of the Czerny-Turner spectrograph. This gives two separate beams and spectrograms for right and left circularly polarized light, i.e. for $\frac{1}{2}(I+V)$ and $\frac{1}{2}(I-V)$ from which the Stokes I and V components can be derived. The width of the entrance slit of the spectrograph was 60 μm ($\widehat{=}$ 0.″5). The spectrograph allows the simultaneous imaging of two separate spectral bands onto the same detector by means of a spectrum cutter. Spectral regions near 615 nm were selected to combine the Fe I 617.3 nm line either with Fe I 615.1 nm or with Fe II 614.9 nm. A Peltier-cooled CCD detector from Wright Instruments Ltd with a Thomson 1024x1024 chip (THX 31156) was used. Short exposure times of 0.1–0.2 s were chosen to obtain high spatial resolution.

Fe I 617.3 has an equivalent width $W_\lambda = 0.67$ pm. It is a pure Zeeman triplet with Landé factor $g = 2.5$. Fe I 615.1 nm (W_λ = 0.45 pm) possesses a complicated Zeeman pattern with $g_{\rm eff}$ = 1.833, while Fe II 614.9 ($W_\lambda = 0.35$ pm) has $g = 4/3$ with two π components at the same position as the σ components. The Fe I lines are from the same multiplet, No. 62. To construct models of small-scale magnetic flux tubes, Kneer et al. (1996) have exploited that these lines are sensitive to temperature variation due to the high ionization degree of iron in the solar atmosphere. On the other hand, the combination of the Fe II line of low magnetic sensitivity with the Fe I 617.3 line with large Landé factor has proved fruitful for separating magnetic and non-magnetic line broadening (cf. Kneer et al. 1996).

The reason for observing plages was that the chance of imaging magnetic elements onto the slit is high there. During the observations, the slit-jaw images in white light, Hα, and Ca K were monitored and recorded. The spectrograms in $\frac{1}{2}(I \pm V)$ were taken from regions with high chromospheric Ca emission, but otherwise at random. In addition several dark CCD frames and some 20 flat field spectrograms from disc centre with varying telescope positions were obtained.

3. Data reduction

We first selected the spectrograms exhibiting the best spatial resolution. These were first reduced in the usual fashion: The average dark signal was subtracted and a gain correction was derived from the flat field spectrograms and was applied. The latter eliminates possible effects from vignetting, varying width of the spectrograph slit along the spatial direction, and dust on the optical surfaces and on the chip. Next, since the two oppositely polarized light beams pass through the spectrograph along slightly different paths, correction for different optical aberrations had to be applied. For this the $\frac{1}{2}(I+V)$ and $\frac{1}{2}(I-V)$ subframes had to be adjusted to have the same orientation of the spatial and the wavelength axes and to have the same spatial and wavelength scale. This is necessary to avoid spurious V signals upon subtraction of the spectrograms. Noise reduction was achieved by low-pass Fourier filtering in wavelength direction and by taking running means in spatial direction over 3 CCD pixels, limiting the spatial resolution to 0.″5.

The addition and subtraction of subframes yielded spectrograms of the Stokes I and V components, respectively, which were normalized to the continuum intensity $I_{\rm C}$. The polarimetric accuracy is of 0.5% of $I_{\rm C}$, essentially due to photon noise and to inaccuracies of the gain corrections. Fig. 1 depicts profiles from regions with strong V signals, i.e. from magnetic regions. The data for the 615.1 and 617.3 lines were taken simultaneously. Those of the 614.9 line stem from a different observing date, thus from a different scenery on the Sun. For comparison, the average I profiles obtained from the flat field spectrograms from disc centre are shown as well. Typical observed profiles of these lines are also shown in Kneer et al. (1996).

From the I profiles we determined the following line parameters: continuum intensity $I_{\rm C}$; line centre residual intensity $I_{\rm lc}$; velocity $v_{\rm I}$ from the position of the line centre; and the full width at half line depression $FWHD$. The values of $v_{\rm I}$ will be given relative to the running mean velocity taken over 5″derived from the position of the minimum intensity $I_{\rm lc}$. In this way small-scale, mainly granular velocities are averaged out and $v_{\rm I}$ is measured relative to the background of the 5 min oscillations. The V profiles yield: the maximum amplitude $V_{\rm max}$ = max(a_b, a_r) with a_b and a_r the unsigned blue and red extrema of the V profile, respectively; the amplitude asymmetry $\delta a = (a_b - a_r)/(a_b + a_r)$; the wavelength separation $\Delta\lambda_V$ of a_r and a_b; and the velocity $v_{\rm zc}$ deduced from the position of the zero crossing of the V profile. Again, $v_{\rm zc}$ is measured relative to the average line centre position, i.e. its running mean over 5″. $I_{\rm lc}$, $v_{\rm I}$, $V_{\rm max}$, $\Delta\lambda_V$, and δa are obtained from parabolic fits about the extrema of the profiles, $v_{\rm zc}$ from a third order polynomial fit about the zero crossing of V. The Stokes V data are determined only at spatial positions where the V signal is sufficiently strong. We chose as a lower limit $V_{\rm max} = 0.02\ I_{\rm C}$, which is well above noise and possible spurious, instrumental V signals.

4. Results and discussion

4.1. Details for line properties for Fe I 617.3

To illustrate observable effects of the presence of small magnetic elements, we first give some detailed results for the 617.3 line from single spectrograms. From the smallest features seen in such spectrograms, we estimate a spatial resolution of 0.″6–1.″0, i.e. we certainly do not yet resolve single flux tubes. The data extracted from the I profiles are plotted in Fig. 2. At the positions with sufficiently strong V signal the curves are fully drawn, they are dotted otherwise. At spatial resolution not better than 0.″5, the magnetic elements do not show up near disc centre by conspicuous continuum intensities. This is known (cf. Kneer & von Uexküll 1991 and references there), but still of some relevance, since Solanki & Briglević (1992) from low spatial resolution V profiles came to the conclusion that magnetic elements, i.e. the flux tubes proper, in plages are noticeably darker than average. Such low intensities were later modeled by Grossmann-Doerth et al. (1994). We shall come back to this point below.

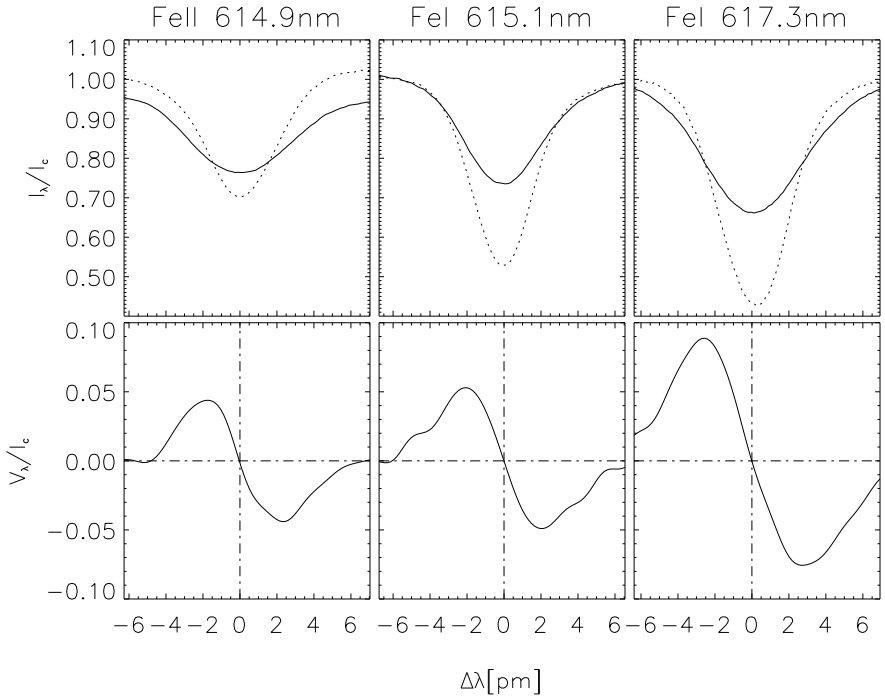

Fig. 1. Stokes I and V profiles observed with high spatial resolution in plages near disc centre, normalized to the local continuum intensity. The V zero crossings have been chosen as reference wavelengths. The data of the Fe I lines are from simultaneous observations. The dotted profiles are from disc centre of the quiet Sun.

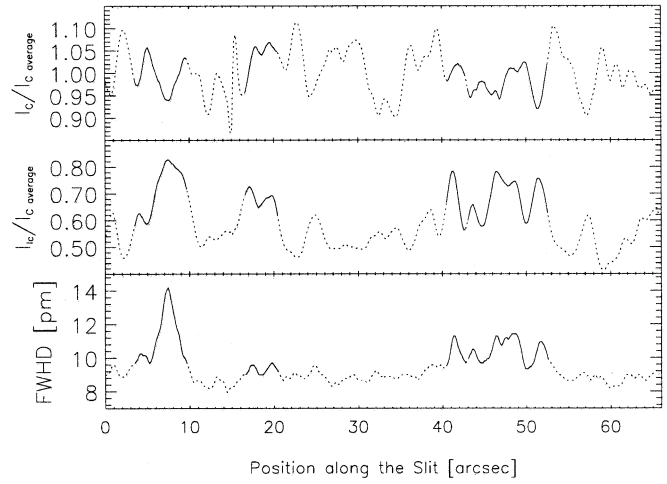

Fig. 2. Properties of the I profiles of the Fe I 617.3 nm line along the spatial position. From top to bottom: continuum intensity I_C relative to the average; line centre intensity I_{lc}; and the full width at half depression $FWHD$. Solid lines: at positions with V signal; dotted lines: otherwise. The large deviations of I_C at the slit position 16–17″ stem from the fiducial mark at the entrance slit of the spectrograph.

Close to the limb, the photospheric facular points in plages appear as bright features. Our observations from the position $\cos\vartheta = 0.28$ (not shown here) show enhancements by 10–15% in the continuum intensity at the same spatial resolution. The maximum continuum intensity always appears about 0.″5 closer to the limb than the maximum V signal.

The relative line centre intensities along the spatial direction are plotted in the second panel of Fig. 2. Obviously, magnetic signals are accompanied by substantial line centre intensity enhancement, which is known as the "gap phenomenon" (cf. Kneer & von Uexküll 1991). The $FWHD$ of the I profiles is increased at positions where magnetic signal occurs and where the line centre intensity is increased (that of the average quiet Sun profile at disc centre (from the flat fields) amounts to $FWHD_{\rm quiet} \approx 9.0$ pm).

Fig. 3 shows the data obtained from the V profiles. The uppermost panel shows the signed extremal amplitude $V_{\rm max}$ at positions where it is larger then 0.02 $I_{\rm C}$. The highest values are above 0.10 $I_{\rm C}$. Comparing these data with the first panel of Fig. 2, one obtains the impression that the strongest V signals occur at positions where $I_{\rm C}$ is lower than average. In the present observations by about 5% at the positions 8″ and 48″. However close inspection of this and other spectrograms shows that this is not regularly the case. Again, we shall expand on this point further below.

In the subsequent panel, the separation $\Delta\lambda_V$ of the position of the V extrema is plotted. The error of the individual values can be estimated from the differences between the fitted and the observed profiles. It amounts to ±0.5 pm. The average $\Delta\lambda_V$ is 12.0 pm with fluctuations between 10.0 and 14.0 pm. Calculations by Amer & Kneer (1993) and Kneer et al. (1996) have shown that this $\Delta\lambda_V$ is much larger than the limit set by the weak field approximation. Using this separation to measure the field strength, one arrives at 135.0 mT on average with fluctuations between 112.5 and 157.5 mT. These values are in good agreement with previous determinations (e.g. Beckers & Schröter 1968, cf. also the references given in Sect. 1). We note however that calculations of both static flux tube models (Kneer et al. 1996) and dynamic models (Grossmann-Doerth et al. 1994) fail to reproduce the separation of the extrema: some additional broadening of the profiles is always needed to obtain the observed $\Delta\lambda_{\rm V}$.

In most cases the V profiles of Fe I 617.3 possess blue-asymmetries near disc centre (panel 3 of Fig. 3), with an av-

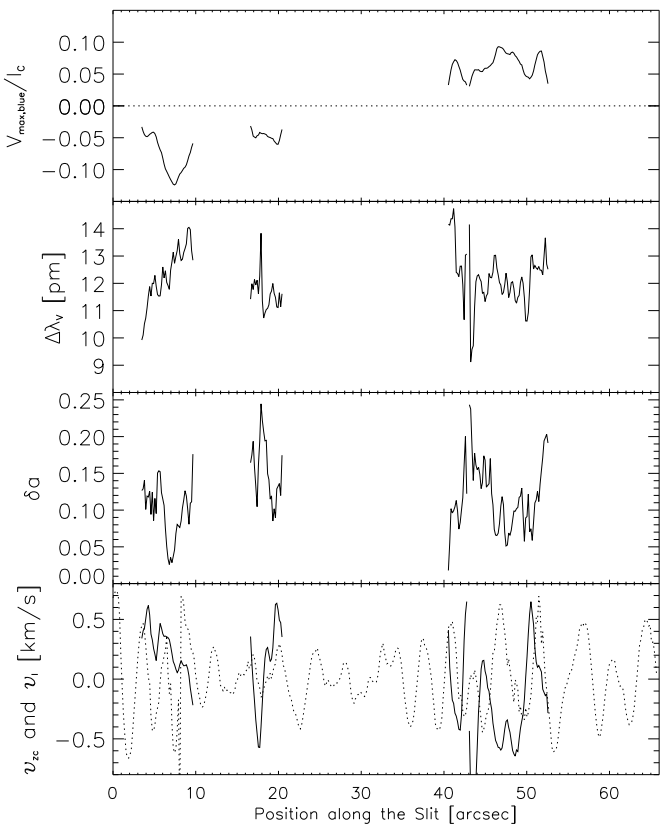

Fig. 3. Properties of the V profiles of the Fe I 617.3 line along the spatial position. From top to bottom: signed extremum of V, separation of the V extrema $\Delta\lambda_V$, amplitude asymmetry δa, velociy v_{zc} of the zero crossing of the V profile (solid lines) in comparison with the velocities v_I (dotted lines) determined from the I profiles. Large-scale motions are subtracted from v_{zc} and v_I.

erage value δa_{av} of 0.11 and fluctuations between 0.0 and 0.25. This confirms earlier results by Amer & Kneer (1993; see also Solanki 1993, 1995, and references therein). The error of individual values is found from $\Delta(\delta a) \approx 1.4\Delta(a_{b,r})/(a_b + a_r)$, where $\Delta(a_{b,r}) \lessapprox 0.01$ is the estimated error of the amplitudes a_b and a_r. With a_b and a_r in the range of 0.05–0.10, we obtain errors of the asymmetry $\Delta(\delta a)$ of about 0.14–0.07, i.e. decreasing with increasing $a_{b,r}$ and of the same order as δa itself.

The bottom panel of Fig. 3 depicts the velocity v_{zc} together with the small-scale granular motions after subtraction of large-scale flows (positive velocities are directed away from the observer). From the difference between the observed and fitted zero crossings, one obtains an error estimate of ± 130 m s^{-1}. The rms value of v_{zc} is 410 m s^{-1} in agreement with the finding of Martínez Pillet et al. (1996), while that of v_I is 280 m s^{-1}. Multiplying the rms value with $\sqrt{2}$ (assuming a Gaussian velocity distribution), one arrives at a macroturbulent parameter $v_{Doppler} = 580$ m s^{-1} for the zero crossing velocity. This falls short by factors of 3–5 of the value needed to fit the V profiles observed with low spatial resolution (cf. Keller et al. 1990, Rüedi et al. 1992). Thus, the high velocities in the magnetized plasma are not (yet) seen. A similar concern was already expressed by Fleck & Deubner (1991). We note, however, that within one magnetic patch of a few arcsec extent, v_{zc} may vary by 1.0–1.5 km s^{-1} (see also Fleck & Deubner 1991 and Volkmer et al. 1995). Also, v_{zc} may exhibit large differences from v_I at the same location. The latter measures, to a large extent, the velocity in the non-magnetic atmosphere surrounding the small-scale flux tubes.

Recently, Steiner et al. (1996) have given a possible solution to the discrepancy between the rather low v_{zc} seen at high spatial resolutions and the high "macroturbulent" velocity derived from low spatial resolution data. Their numerical simulations of the dynamics of small-scale magnetic fields embedded in the granular flow exhibit strong vertical velocity gradients and shocks within the magnetic element. In such scenarios, the velocities are intrinsically hidden from high angular resolution observations: radiative transfer effects average out the contributions to v_{zc} from widely differing velocities along the line of sight and the V profile exhibits a large separation $\Delta\lambda_V$ of the extrema.

4.2. Correlations between profile parameters of the Fe I 617.3 line

We now combine the data from several Fe I 617.3 nm line spectrograms and give some examples of correlations among profile parameters in regions with sufficiently strong V signal. This gives *typical*, average line properties and their fluctuations from high resolution observations. We present these data because they give constraints for modeling small-scale magnetic structures together with their ambient atmosphere.

In Fig. 4, the pairs V_{max} – I_C, $\Delta\lambda_V$ – V_{max}, and $\Delta\lambda_V$ – $FWHD$ are plotted. With the achieved resolution, the presence of small-scale flux tubes does not noticeably change the continuum intensity I_C at disc centre. The upper panel of Fig. 4 shows that, at positions with V signal, I_C fluctuates by $\pm 5\%$ about the average $\bar{I}_C$ calculated from the continuum intensities at all positions. The mean continuum intensity, taken only from positions with V signal, amounts to $1.0\bar{I}_C$. However, a weak relation between V_{max} and I_C with a correlation coefficient -0.57 is present: strong V signal occurs preferentially in "dark" areas. Our limited spatial resolution does not allow us to discriminate between the two possibilities: either the "low" continuum intensity stems mainly from the ambient medium, e.g. from intergranular lanes, or the "low" intensity is an intrinsic property of the flux tubes in plages, as deduced by Solanki & Briglević (1992). Kneer et al. (1996) estimate from their flux tube models that the area filling factor (at $\tau_{cont} = 1$, or z = 0) at positions with highest V signal in the present observations is 25–50%. Thus, a substantial part, if not most, of the continuum radiation does indeed come from the ambient, non-magnetic atmosphere. However, Grossmann-Doerth et al. (1994) have shown that models with low intensity are feasible. It would be of interest to know how such models compare with observation when the continuum intensity is averaged over areas that include the surrounding, non-magnetic atmosphere.

V_{max} depends on the internal flux tube structure, essentially its run of temperature (cf. Kneer et al. 1996), *and* on the total

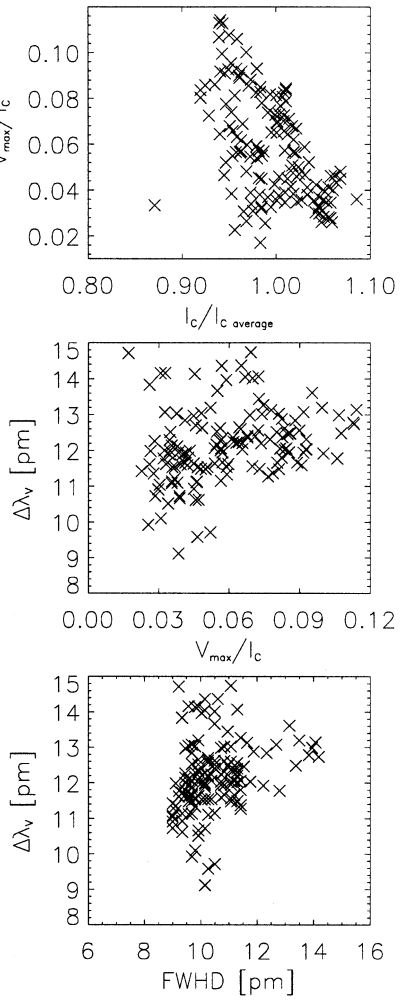

Fig. 4. Relationships between various profile parameters of Fe I 617.3

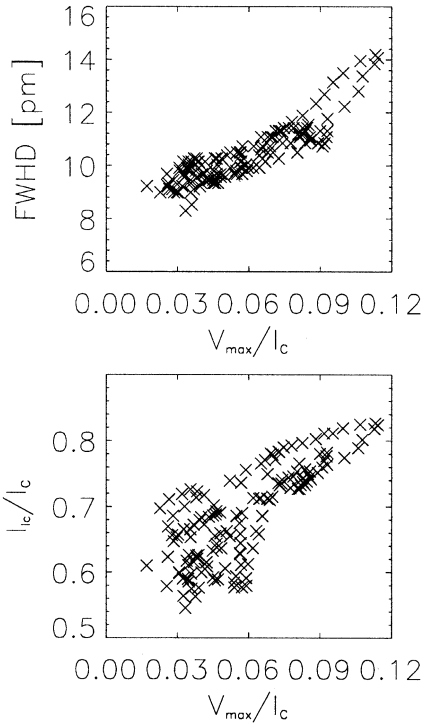

Fig. 5. Relationships between the profile parameters $V_{\rm max}$, $FWHD$, $I_{\rm lc}$ of Fe I 617.3.

flux within the resolution element, i.e. the filling of the considered area with magnetic structure (middle and lower panels of Fig. 4). Likewise, the line width $FWHD$ is a function of the temperature and density structure inside *and* outside the flux tubes and of the magnetic flux within the resolution element. On the other hand, the separation of the V extrema, $\Delta\lambda_{\rm V}$, does not depend on the amount of light from non-magnetic regions, i.e. the filling factor: It is determined solely by the flux tube properties and their fluctuations within the resolution element. Thus, $\Delta\lambda_{\rm V}$ is not expected to be related to the other parameters.

Parameter pairs with fair to high correlations are depicted in Fig. 5. These are the combinations $FWHD$ – $V_{\rm max}$, $I_{\rm lc}$ – $V_{\rm max}$, and $FWHD$ – $I_{\rm lc}$. All three parameters have similar dependencies on temperature/density, total flux, and contribution from non-magnetic areas. At the extreme of low spatial resolution and low detected flux only averaged V profiles carry information about flux tubes, again averaged over various thermal, magnetic, and dynamic states. With increased resolution, the properties of the I profiles may serve, in addition to the V profiles, to deduce the structure of flux tubes and of their neighbourhood.

The flux tube velocities $v_{\rm zc}$ are uncorrelated or only weakly correlated with $V_{\rm max}$, $\Delta\lambda_{\rm V}$, and δa, so we comment upon this point only briefly. It appears reasonable that the amplitude of the V signal, i.e. essentially the magnetic filling, has no influence on the measurement of the velocity of the magnetic plasma. Remarkably, $v_{\rm zc}$ does not depend on the separation of the V extrema $\Delta\lambda_{\rm V}$. For strong magnetic fields, $\Delta\lambda_{\rm V}$ may be used as a (zeroth order) proxy of the field strength. It does depend, however, on the line width and thus on unresolved velocities, as noted above. The more vigorous the dynamical processes are, the higher are their influence on the separation $\Delta\lambda_{\rm V}$. Dynamic model calculations by Steiner et al. (1996) give strong blueshifts of the V profile simultaneously with wide separations of the V extrema.

There is a very weak tendency (correlation coefficient 0.43) for increased blue-asymmetry with increased downflow. This contradicts the siphon flow model of Degenhardt & Kneer (1992) in which an enhanced blue-asymmetry of the V profiles is produced by upflows in flux tubes. Yet data with higher signal/noise are needed to settle this point.

Consistent with the results of Fig. 5, parameters as $FWHD$ and $I_{\rm lc}$ are uncorrelated with $v_{\rm zc}$ in the same way as $V_{\rm max}$.

4.3. Correlation of line parameters among different lines

Some relations of line parameters among different lines appear reasonable and expected, so we will not show them as figures. Some typical parameters of the I and V profiles may be extracted from Fig. 1. First, the values of $V_{\rm max}$, $I_{\rm lc}$, and $FWHD$ of

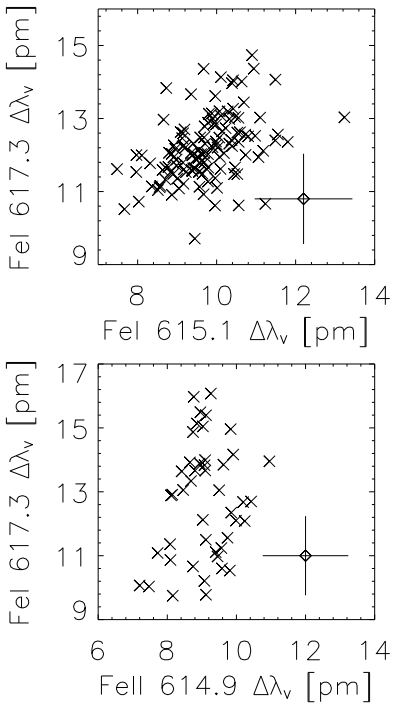

Fig. 6. Separation $\Delta\lambda_V$ of V extrema of the line pairs Fe I 617.3 – Fe I 615.1 and Fe I 617.3 – Fe II 614.9. The large crosses indicate the 1σ errors of the individual determinations of $\Delta\lambda_V$.

two simultaneously observed lines are correlated: in any pair of the observed spectral lines the same magnetic elements are seen and essentially the same mixture of magnetic and non-magnetic areas contributes to the signals. Second, the velocities v_{zc} are correlated within the error bars of the individual measurements. Finally, the asymmetries δa of two lines are uncorrelated, simply because the 1σ errors of the individual values are as large as the values themselves.

The separation of the V extrema $\Delta\lambda_V$ of the two line pairs Fe I 617.3 – Fe I 615.1 and Fe I 617.3 – Fe II 614.9 are shown in Fig. 6, along with the $\pm1\sigma$ error bars of the individual determinations (large crosses). The correlation coefficients are low: 0.42 for 617.3/615.1 and 0.20 for 617.3/614.9, due to the errors of the individual determination. However, the wide fluctuations of the $\Delta\lambda_V$ values of Fe I 617.3 and Fe I 615.1 are significant and indicate a large variability of magnetic flux tubes, or of clusters of flux tubes within the spatial resolution element. Further work is required to settle this point. The Fe II 614.9 line exhibits the smallest fluctuations of $\Delta\lambda_V$, presumably due to its low Landé factor, which is about 1/2 of that of the Fe I 617.3 line.

5. Conclusions

The continuum intensities of small-scale flux tubes averaged over the magnetic elements and the surrounding area is $\pm5\%$ of the quiet Sun intensity, almost independently of the magnetic flux contained in the area of the spatial resolution element. There exists, however, a small tendency for lower intensities at sites with strong V signal.

The large macro-velocities of 1.5–3 km s^{-1} in the magnetized plasma, often adopted to fit Stokes V profiles from models to the observations, are not yet seen with the present resolution. The large width of the observed V profiles thus remains an unresolved puzzle and an important issue for further high spatial resolution observations. We note also, that, at sufficiently high spatial resolutions, the I profiles become very wide. This can partly be ascribed to magnetic splitting, but an additional, yet unspecified broadening mechanism also appears necessary for the I profiles (cf. Kneer et al. 1996).

The large fluctuation of the separation of the V extrema indicates a wide variety of the structure and dynamics of magnetic elements. This finding requires an explanation in terms of highly dynamic flux tubes interacting with the surrounding medium at all atmospheric and subphotospheric levels. Rüedi et al. (1992) found very different magnetic field strengths of 50–165 mT (at z = 0) in solar plages from infrared observations of low spatial resolution. Although they were able to reproduce the observed V profiles with static flux tube models, a macro-velocity of 2 km s^{-1} was still needed to cope with the width of the profiles, which is again uncomfortably large for *static* atmospheres. Kneer & Stolpe (1996) have suggested a picture of substructure on scales smaller than those presently resolved, with stochastic behaviours of both the magnetized plasma and the ambient gas. Similar interpretations have been presented by Domke & Pavlov (1979). Recent developments by Sánchez Almeida et al. (1996) of modeling the transfer of the Stokes vector in micro-structured magnetic elements imbedded in an intense flow field appear successful and promise a new view of small-scale magnetic structures in the solar atmosphere. A further fruitful route of investigation is the numerical modeling of small-scale magnetic field dynamics as done e.g. by Steiner et al. (1996). There, the large spatial and temporal variation of the (thermo-) dynamic and magnetic field parameters can possibly explain the rather small velocities v_{zc} in the magnetic plasma when observed with high spatial resolution on the one hand, and the needs for V and I profile broadening in addition to Zeeman broadening on the other. In the framework of such models, very large separations of the V extrema, as found in the present investigation and in Amer & Kneer (1993) are the result of large velocity gradients along the line of sight, as occurring e.g. in shocks. In any case, our results emphasize that small-scale magnetic elements are dynamic structures which interact dynamically with their ambient medium.

Although it is laborious to perform the observations and the data analysis, and combinations of only a small number of spectral lines, 2 – 6, can be observed simultaneously with high spatial resolution at this state of the art, such observations are important in giving constraints on models of structure and dynamics in and around flux tubes. It is thus worthwhile to continue the effort.

Acknowledgements. We thank Dr. M. Schüssler for valuable comments on the manuscript and Dr. F. V. Hessman for help with the En-

glish. The Gregory Coudé Telescope is operated by the Universitäts-Sternwarte Göttingen at the Spanish Observatorio del Teide/Tenerife of the Instituto de Astrofísica de Canarias.

References

Amer M.A., Kneer F., 1993, A&A 273, 304
Beckers J.M., Schröter E.H., 1968, Solar Phys. 4, 142
Degenhardt D., Kneer F., 1992, A&A 260, 411
Domke H., Pavlov G.G., 1979, Ap&SS 66, 47
Fleck B., Deubner F.-L., 1991, Observations of Waves and Oscillations in Solar Magnetic Fluxtube Concentrations. In: Ulmschneider P., Priest E.R., Rosner R. (eds.) Proc. Internat. Conf., Heidelberg, 5–8 June 1990, Mechanisms of Chromospheric and Coronal Heating. Springer, Heidelberg, p. 19
Grossmann-Doerth U., Knölker M., Schüssler M., Solanki S.K., 1994, A&A 285, 648
Keller C.U., von der Lühe O., 1992, A&A 261, 321
Keller C.U., Solanki S.K., Steiner O., Stenflo J.O., 1990, A&A 233, 583
Kneer F., Stolpe F., 1996, High Resolution Observations of Small-Scale Magnetic Elements and Interpretation. In: Stenflo J.O., Nagendra K.N. (eds.) Proc. Internat. Conf., Solar Polarization, Solar Phys. 164, 303
Kneer F., von Uexküll M., 1991, A&A 247, 556
Kneer F., Schmidt W., Wiehr E., Wittmann A.D., 1987, Mitt. Astron. Ges. 68, 181
Kneer F., Hasan S.S., Kalkofen W., 1996, A&A 305, 660
Martínez Pillet V., Lites B.W., Skumanich A., 1996, ApJ, submitted
Rüedi I., Solanki S.K., Livingston W., Stenflo J.O., 1992, A&A 263, 323
Sánchez Almeida J., Landi Degl'Innocenti E., Martínez Pillet V., Lites B.W., 1996, ApJ, in press
Solanki S.K., 1993, Space Sci. Rev. 63, 1
Solanki S.K., 1995, Magnetic Field Measurements in the Infrared. In: Kuhn J., Penn M. (eds.) Proc. 15th Sacramento Peak Workshop, 1995, Infrared Tools for Solar Astrophysics: What's Next? Sunspot, NM, World Scientific, p. 341
Solanki S.K., Briglević V., 1992, A&A 262, L29
Solanki S.K., Stenflo J.O., 1984, A&A 140, 185
Solanki S.K., Stenflo J.O., 1985, A&A 148, 123
Steiner O., Grossmann-Doerth U., Schüssler M., 1996, Solar Phys., in press
Stenflo J.O., 1973, Solar Phys. 32, 41
Stenflo J.O., 1994, Solar Magnetic Fields — Polarized Radiation Diagnostics. Kluwer, Dordrecht
Ulmschneider P., Priest E.R., Rosner R. (eds.), 1991, Chromospheric and Coronal Heating Mechanisms. Springer, Berlin
Volkmer R., Kneer F., Bendlin C., 1995, A&A 304, L1

This article was processed by the author using Springer-Verlag LaTeX A&A style file *L-AA* version 3.